ANALYSIS OF THE GRAIN BOUNDARY MICROSTRUCTURE AND DEGRADATION IN A GAS TURBINE BLADE

АНАЛИЗ МИКРОСТРУКТУРЫ ГРАНИЦ ЗЕРЕН И ДЕГРАДАЦИИ В ЛОПАТКЕ ГАЗОВОЙ ТУРБИНЫ

Davydov D.I., Kazantseva N.V., Vinogradova N.I., Ezhov I.V., Stepanova N. N.
Institute of Metal Physics of Ural Branch of Russian Academy of Sciences, Ekaterinburg, Russia

Abstract: *We studied the different parts (lock and feather) of Inconel 738C gas turbine blade, which were cut from the working turbine blade after long operation and recovery heat treatment. Undesired phases such as TCP phase (sigma phase) and some of continuous carbides such as $M_{23}C_6$ in the grain boundary are found. The presence of $M_{23}C_6$ carbides in studied samples testifies to the diffusion process of decomposition of MC carbide and the associated softening of the alloy. The appearance of sigma phase leads to embrittlement of the alloy. Generation of these specifications in the structure results in degradation of metallurgical and mechanical properties of the blade and eventually its destruction.*

***KEYWORDS**: NICKEL SUPERALLOYS, MICROSTRUCTURE, DEGRADATION, PHASES, GAS TURBINE BLADE*

1. Introduction

During the exploitation, the gas turbine blades and other components of turbine are subject to wear and damage. Operation aggressive environment, high mechanical and thermal stresses are the main factors, which influence lifetime of the main components of a gas turbine. After a prolonged service, moving blades undergo mechanical and structural degradation and show a decrease in the creep strength, fatigue, impact, and corrosion resistance. Microstructural degradation is considered as a major course for replacement or recovering of gas turbine blades [1]. Because of that the microstructural analysis of the degree of degradation and estimation of the residual lifetime of the blades are very important.

The nickel based super alloys mechanical properties depends on the volume fraction, size, form and composition of both the gamma prime phase (Ni_3Al) and grain-boundary MC carbides. Increase of heat resistance in the nickel super alloys is realized due to strengthening the grain boundaries with elements such as B and Zr, which reduce the probability of TCP phase formation and carbide transformation, which lead to reduce the strength of the alloy. Microstructural changes include the coarsening of the γ'-phase particles, change of the grain boundary morphology and the chemical composition of the carbide phase, as well as the precipitation of brittle intermetallic TCP phases, for example, σ phase [2]. Loss of long-term strength provides the growth of internal stresses, which leads to the grain boundary destruction of the alloy. Although most microstructure changes can be restored by special heat treatments, many structural defects can be persist after them [3, 4].

The Inconel 738C (IN738) super alloy, developed in 1968, is one of the important nickel based super alloys. This alloy shows the improved creep, hot corrosion, and oxidation resistance and is used in land-based gas turbines [5]. IN738 is used in manufacturing of gas turbine, jet engines, nuclear reactors, high-pressure vessels due to the high stability of its mechanical properties at elevated temperatures (up to 800 °C). The main phases of IN738 are nickel solid solution (gamma phase), a hardening intermetallic compound Ni_3Al (gamma prime phase), carbide and boride phases (MC and Cr_3B_2) [6].

The aim of work is to study the structure of the cast polycrystalline gas turbine blade made from Inconel 738C super alloy after long time exploitation and recovering heat treatments.

2. Experimental procedure

Chemical composition of Inconel 738C super alloy is presented in Table 1. We study the samples cut from the hottest and the most stressed part of the feather of gas turbine blade taken from the stationary gas turbine plant as well as the sample cut from the lock part of the blade. Standard two steps recovering was done at 1100°C for 2 h following by aging at 840°C for 24 h. Air cooling was done after every step of heat treatments.

Table 1. Chemical composition of Inconel 738C, wt.% [5].

Ni	Cr	Co	Mo	W	Ta	Ti	Al	other
base	16	8.51	1.7	2.6	1.7	3.4	3.4	Nb, Zr, C, B

Structural studies were done with an optical microscope Micromed MET, a JEM-200CX transmission electron microscope and a scanning electron microscope JSM 6490 with the Oxford Inca energy dispersive and wave microanalysis. X-ray diffraction analysis was done with the X-ray diffractometer DRON-3 used the CuKα radiation.

3. Results and discussion

Optical study reveals the change in the microstructure of both feather and lock samples (Fig.1). The grain size in the samples changes from 100 up to 800 micrometers. Carbides are observed in both samples inside the grains and along their boundaries. Intergranular carbide precipitations have a well-defined globular shape which is typical for MC carbide. Grain-boundary carbides have the globular and elongated shapes. Elongated carbides are supposed to be the $M_{23}C_6$ carbides, which completely cover the grain boundaries.

It is known that the IN738 is an alloy with MC type carbide hardening based on Nb, Ti, W chemical elements. Doping with the boron is also used. To increase the heat resistance of the material, the grain-boundary carbide precipitations should be globular shape, have a size of 1 μm or less, and be evenly distributed along the grain boundaries without the formation of a continuous grid [6].

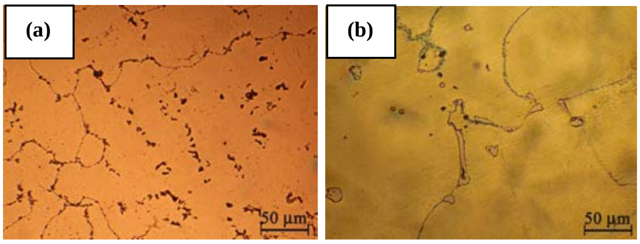

***Fig.1.** Microstructure of the studied gas turbine blade, optical microscopy: a- feather; b- lock*

TEM study of the γ'-phase morphology in hottest and most stressed part of the feather can be seen in Figure 2. Bimodal distribution of the γ'-phase particles in cuboid-shaped particles with size of about 350 nm and spherical-shaped particles with a diameter of about 50 nm is observed.

One can see that the recovering heat treatment eliminates the planar defects (stacking faults, dislocations) inside of the γ'-phase cuboids formed during long-term operation of the blade (Fig.2).

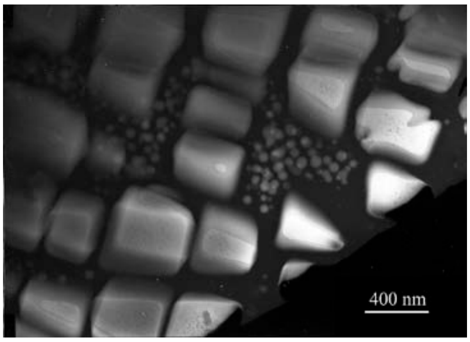

Fig.2 *Structure of the feather, TEM, the dark-field image in γ′-phase reflex*

Figure 3 shows the carbide transformation in the lock part of the gas turbine blade. It can be seen that partial dissolution of MC carbides and precipitation of a large number of $M_{23}C_6$ carbides occur during the exploitation. Recovering heat treatment according to the standard regime does not lead to the dissolution of $M_{23}C_6$ carbides. $M_{23}C_6$ carbides are mainly concentrated on the grain boundaries (Fig. 3b). Some of $M_{23}C_6$ carbides are observed on the structural defects in the grain (Fig. 3a).

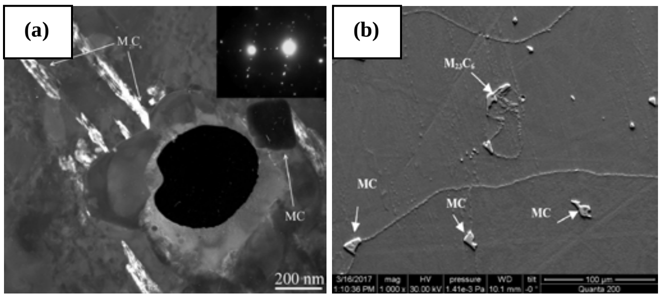

Fig.3. – Structure of carbide phases, lock,: a- TEM, the dark-field image in $M_{23}C_6$ reflex; b- SEM

The same carbide transformations one can see in the feather part of the blade (Fig.4). Intragrain MC carbide has a shape close to cubic one (Fig. 4a). $M_{23}C_6$ carbides are observed on the grain boundaries and have the elongated form (Fig.4b). Chemical composition of the carbides is shown in Tables 2-3 and in Figures 5-6. In the lock part of the blade, secondary $M_{23}C_6$ carbides, which are close to the MC carbide, have high content of nickel, chromium and cobalt. Intragrain MC carbides have high content of titanium, niobium and tantalum and practical absence of chromium (Table 2).

In contrast to the MC carbides of the locking part, the MC carbides in the sample cut from the feather of the blade contain in two time smaller amount of tantalum. $M_{23}C_6$ carbides located along the grain boundaries have approximately the same chemical composition as in the $M_{23}C_6$ carbides of the lock part (Table 3).

In addition to carbides in this part of the blade, precipitations of TCP σ-phase inside the grains are found (Fig.7). Chemical composition of this phase is close to MC carbide, however high nickel content is found in this phase (Table 2)

In comparison with the sample cut from the lock part of the blade, γ- (nickel solid solution) and γ′ (Ni_3Al) -phases in the feather part of the blade have the less nickel content and higher percentage of tantalum and molybdenum (Tables 1-2).

The results of X-ray diffraction analysis support the structural studies (Fig. 8). X-ray diffractograms show the diffraction lines of the γ/γ′-phases and carbides in the lock part of the blade (Fig. 8a). In the structure of the sample cut from the feather part of the blade, in addition to the γ/ γ′ -phase and carbide diffraction lines, the diffraction lines of the TCP σ- phase are observed (Fig. 8b).

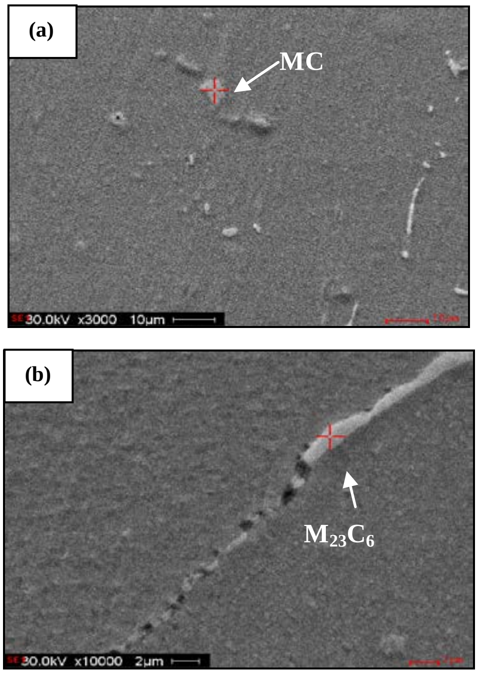

Fig.4 *Structure of carbides (pointed by cross), feather: a- MC; b- $M_{23}C_6$*

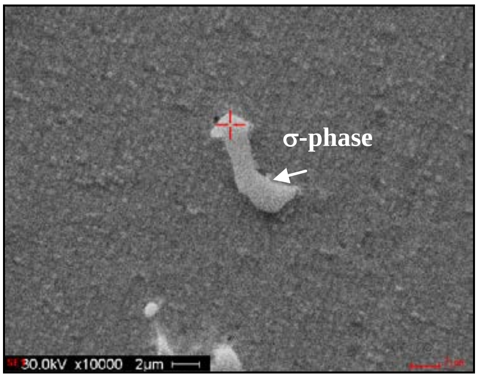

Fig. 7. *Structure of σ-phase in the feather, SEM*

During the operation time, gas turbine blades can be compressed, stretched, twisted or bended. This changes the aerodynamic characteristics and coordination of the turbine stages. Maximum tensile stresses are achieved in the surface layer of the feather of the gas turbine blade [7]. In differ from the feather of the gas turbine blade, the lock of the gas turbine blade undergoes only thermal influences [4]. In order to reduce the rate of diffusion processes in the solid solution and the exchange processes between the solid solution and the hardening γ′-phase, the high-temperature nickel alloys are especially alloyed with chromium, tungsten and molybdenum. Gorsky explained the main course of the concentration change in the stressed alloy. He call it the effect of ascending diffusion [8]. Change in the chemical composition of the feather part of the nickel gas turbine blade after the long exploitation was also found in [9]. It was observed the decreasing of the nickel content in the surface layer of the feather in compare with inner part of the feather or lock part of the gas turbine blade [9].

In this study, we researched the surface of the gas turbine blade. The change in the chemical composition of the hottest and stressed feather part of the blade indicates the degradation of both the solid solution and the strengthening phase.

The formation of TCP phases (σ, μ, Laves phases), as well as of M_6C or $M_{23}C_6$ carbides, leads to softening of the alloy and it is undesirable in high-temperature nickel alloys [4].

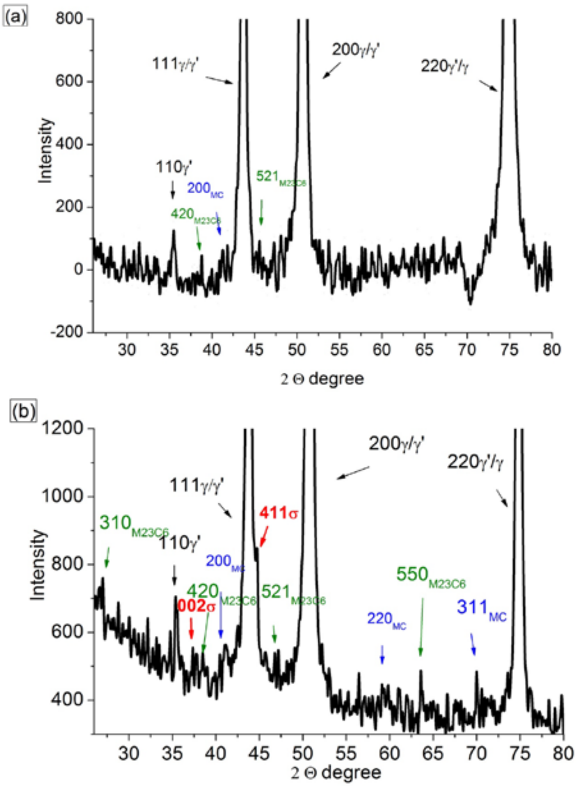

***Fig.7**. X-ray diffractograms of studied alloys: a- lock; b- feather*

Usually carbides in high-temperature nickel alloys are resistant to high temperatures. Grain boundary $M_{23}C_6$ carbides have a solvus of about 1025 °C and dissolve at higher temperatures. MC carbides are resistant up to ~1235 °C [7]. Thermal stability and shape of the carbides also depends on the carbon content in the alloy. Redistribution of the alloying elements in primary MC carbides and in the surrounding carbide zones may occur under high temperature and stress. Precipitation of primary MC carbides during solidification is usual for Inconel 718 [10]. Serrated network of grain-boundary nano-scale $M_{23}C_6$ carbide and M_5B_3 boride precipitates were found in standard heat-treated commercial nickel base superalloy Inconel 738 [11]. Grain-boundary $M_{23}C_6$ carbides were observed in Inconel 738C after long time annealing at 850 °C for 100 hours [12].

Size and position of the $M_{23}C_6$ carbides in our case allow us to suggest its formation under exploitation time. Standard recovering heat treatment at 1100 °C should dissolve the $M_{23}C_6$ carbides. However, TEM studies (Fig 3) and high concentration of Cr in the grain-boundary carbides detected using X-ray microanalysis (Tables 1-2) give an experimental evidence that these carbides are secondary $M_{23}C_6$ carbides. It also means that our grain-boundary $M_{23}C_6$ carbides form under grain-boundary MC carbide transformation; to recover the chemical composition of the MC carbide phase, the alloy should be heated up to γ-phase melting temperature.

It is known that discrete grain-boundary $M_{23}C_6$ carbides improve creep life and ductility, but continuous network grain-boundary $M_{23}C_6$ carbide is the place for future destruction of the nickel heat temperature alloys because they promote crack blunting due to their effectiveness as dislocation sources [13]. In our case, the carbide network precipitated along the grain boundaries diverts the chromium from the solid solution that promotes the decrease of it oxidation and hot corrosion resistance and weakens the border regions.

Conclusion

Standard recovering heat treatment of the Inconel 718C gas turbine blade after long time operating does not lead to a complete restoration of the structure. Such kind of temperature treatments allows us to restore the structure of the hardening intermetallic γ′-phase. However, the presence in the structure the large number of continuous network of grain-boundary brittle $M_{23}C_6$ carbides and TCP σ- phase change the chemical composition of the γ/γ′- phases. This fact may testify about degradation process in the gas turbine blade; it leads to a significant decrease in the strength characteristics of the material at elevated temperatures and limits the service life of the blade.

Acknowledgments

The research supported by the grant from the Russian Science Foundation No 15-12-00001.

References

1. A. Luna Ramírez, J. Porcayo-Calderon, Z. Mazur, V. M. Salinas-Bravo, and L. Martinez-Gomez, Microstructural Changes during High Temperature Service of a Cobalt-Based Superalloy First Stage Nozzle // Advances in Materials Science and Engineering, 2016. Vol. 2016, p.1-7.
2. E. B. Chabina, E.V. Filonova, B.S.Lomberg, M.M. Bakradze Structure of contemporary deformed nickel alloys / All Materials. 2012, No 6, p. 1-11.
3. M. Zielinska, J. Sieniawski, M. Yavorska, M. Motyka Influence of chemical composition of nickel based superalloy on the formation of aluminide coatings // Archives of metallurgy and materials, Vol. 56, Issue 1, 2011, P.193-197.
4. Superalloys II / Ed. C.T. Sims, N.S. Stoloff, W.C. Hagel, John Wiley and Sons Ltd, United States, 1987, 384 p
5. A.K. Koul, J-P. Immarigeon, R. Castillo, P. Lowden and J. Liburdi, Rejuvenation of service-exposed in 738 turbine blades / Superalloys-1988, Edited by S. Reichman, D.N. Duhl, G. Maurer, S. Antolovich and C. Lund, The Metallurgical Society, 1988, P.755-764.
6. P. Jonšta, K. Konečná, R. Heide, M. Gabčová, Z. Jonšta Microstructural analysis of a cast variant of nickel superalloy Inconel 738LC after high temperature exposition // Metall-2011**,** 2011, Vol.5.18 - 20., P. 1-8.
7. V.Kanaikin, A. Matvienko Damage and destruction of blades of gas pumping units, Ekaterinburg, 2000, 179p.
8. W.S. Gorsky Phys. Zheitschrift Sowjet, 1935, V.8, p.443.
9. N.V.Kazantseva, A.V.Korolev, D.I.Davidov, N.N.Stepanova, N.I.Vinogradova, M.B. Rigmant, Concentration inhomogeneity in the turbine blade received from the nickel superalloy // Metallography, 2013, 4, P.18-24
10. A. Mitchell, A.J. Schmalz, C. Schvezov and S.L. Cockcroft The Precipitation of Primary Carbides in Alloy 718- Superalloys 718, 625,706 and Various Derivatives/ Edited by E.A. Loria, The Minerals, Metals & Materials Society, 1994, p.65-78
11. Huai-Ruo Zhanga ; O. A. Ojoa Cr-rich nanosize precipitates in a standard heat-treated Inconel 738 superalloy// Philosophical Magazine, 2010, 90: 6, p.765- 782.
12. P.Jonšta, K. Konečná, R. Heide, M.Gabčová, Z. Jonšta Microstructural analysis of a cast variant of nickel superalloy inconel 738LC after high temperature exposition / Proc. of conference Metal 2011, Brno, Czech Republic, p.1-8
13. Seong Sik Hwang, Yun Soo Lim, Sung Woo Kim, Dong Jin Kim, and Hong Pyo Kim. Role of grain boundary carbides in cracking behavior of ni base alloys // Nuclear engineering and technology, vol.45 no.1, 2013, p.73-80

Table 2 – Chemical content of different phases in the lock part of the blade, wt.%, SEM

Phases/Elements	Al	Nb	Mo	Ti	Cr	Fe	Co	Ni	Ta	W, Zr
MC	0,53	13,85	2,35	23,38	1,73	0,7	1	5,17	44,25	5,08
$M_{23}C_6$	2,19	1,49	2,52	3,58	16,17	0,7	8,24	58,1	2,76	2,24
γ - phase	2,05	1,56	1,86	3,28	15,32	0,73	7,94	59,54	3,93	2,01
γ′- phase	2,15	2,16	2,40	4,09	14,63	0,99	7,21	56,85	4,86	3,31

Table 3 – Chemical content of different phases in the feather part of the blade, wt.%, SEM

Phases/Elements	Al	Nb	Mo	Ti	Cr	Fe	Co	Ni	Ta	W, Zr
MC	0,52	19,07	14,79	22,59	2,32	-	0.92	6,67	21,06	2.69
$M_{23}C_6$	2,27	2,5	2,97	4,36	13,62	0,22	7,72	56,95	4,32	0,82
γ - phase	2,26	1,32	4,75	3,28	15,47	0,17	8,19	56,67	3,39	1,08
γ′- phase	2,01	1,27	3,16	3,4	14,4	0,62	7,93	54,27	5,14	0,81
σ-phase	0,67	15,78	11,64	19,83	4,27	0,19	1,72	12,37	21,94	1,49

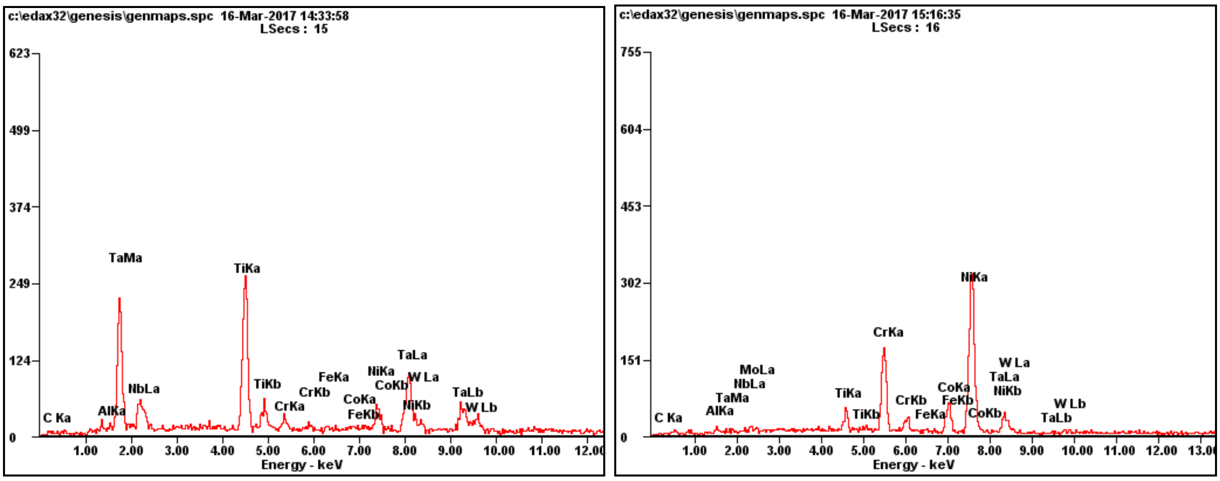

Fig.5. – EDX spectrum of carbide phases, lock part of the blade: a- MC; b- $M_{23}C_6$

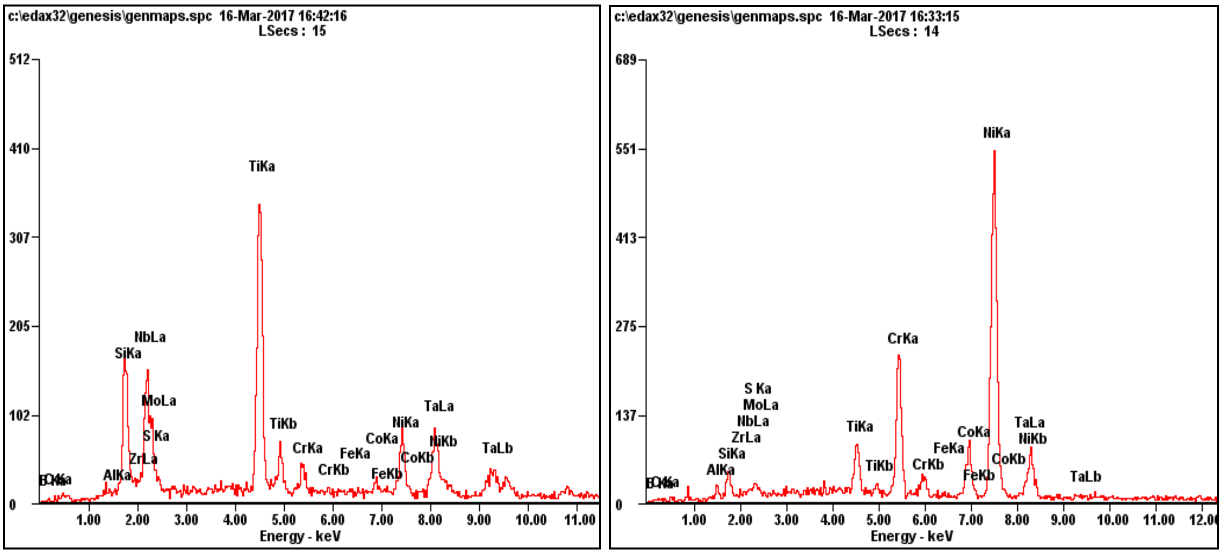

Fig.6. – EDX spectrum of carbide phases, feather part of the blade: a- MC; b- $M_{23}C_6$